# Potential cIBR-Conjugated PLGA Nanoparticles for Selective Targeting to Leukemic Cells

Rungsinee Phongpradist, Sawitree Chiampanichayakul, Singkome Tima, Teruna J. Siahaan,
Cory J. Berkland, Songyot Anuchapreeda, Chadarat Ampasavate

*Abstract*—The expression of LFA-1 diverges from the physiological condition, thus active targeting carrier can provide the benefits from difference into LFA-1 expression in various conditions. Here, the selectivity of cIBR-conjugated nanoparticles (cIBR-NPs), in terms of uptake, was investigated using PBMCs, Mixed PBMC-Molt-3 cells and Molt-3 cells. The expressions of LFA-1 on Molt-3 cells, from flow cytometry and Western blot, possessed the highest level whereas PBMCs showed the lowest level. The kinetic uptake profiles of cIBR-NPs were obtained by flow cytometry, which the degree of cellular uptake presented a similar trend with the level of LFA-1 indicating the influence of LFA-1 expression on the cellular uptake of cIBR-NPs. The conformation of LFA-1 had a slight effect on the cellular uptake of cIBR-NPs. Overall we demonstrated that cIBR-NPs enhanced cellular uptake and improved the selectivity of drug carriers to LFA-1 on the leukemia cells, which related with the order of LFA-1 expression.

*Keywords*—cIBR, LFA-1, Molt-3, PBMCs

## I. INTRODUCTION

ACTIVE targeting is the method of targeting therapy that is becoming an interesting therapeutic strategy for treating cancers. It takes advantage from the different level of specific receptor between targeted and untargeted cells. The crucial constituent of active targeting carrier may be classified into three parts; targeting moiety, targeted receptor, and the suitable carrier. To achieve the active targeting carrier, targeting moiety, which selectively binds to the targeted receptor is attached to the surface of the carrier to improve its selectivity. The targeting moiety performs as a navigator for the carriers, to deliver drug carriers to the targeted cells through molecular recognition such as receptor-ligand or antigen-antibody interaction rather than the physical characteristics of the nanoparticles. The level of receptor plays an important role in the selectivity of the active targeting carrier. For the targeted cell, the level of targeted receptor must significantly differ from the normal cells. To fabricate the targeted drug delivery system for cancer treatment, the targeted receptors that are preferentially expressed on tumor cells are carefully selected.

Rungsinee Phongpradist is with the Department of Pharmaceutical Sciences, Faculty of Pharmacy, Chiang Mai University, 50200 Thailand (phone: 6685-394-4311; e-mail: auan_rx@hotmail.com).
Corresponding authors
Songyot Anuchapreeda is with the Division of Clinical Microscopy, Department of Medical Technology, Faculty of Associated Medical Sciences, Chiang Mai University, 50200 Thailand (phone: 6685-394-9237; e-mail: sanuchapreeda@gmail.com).
Chadarat Ampasavate is with the Department of Pharmaceutical Sciences, Faculty of Pharmacy, Chiang Mai University, 50200 Thailand (phone: 6685-394-4360; email: aimchadarat@windowslive.com)

Polymeric nanoparticles, with biodegradability and biocompatibility, have extensively served as carriers for anticancer agents by providing greater efficiency, controlled release, and less harmful properties than the naked-conventional drugs.

For leukemic cells, there are many markers or receptors that can be used as a targeted receptor. The selection of the targeted marker requires careful investigation due to the presence of different markers in each leukemic cell type. For example, leptin receptor [1], FMS-like tyrosine kinase 3 [2], [3], CD163 [4], [5], IL-2 receptors [6]. One such candidate for the targeted receptor is the lymphocyte function associated antigen-1 [7], since an overexpressing of LFA-1 was reported in certain leukemia cells [8], [9]. According to our previous study, LFA-1 was used as a targeted receptor on four types of leukemic cell lines and cIBR-conjugated PLGA (poly (lactic-co-glycolic acid) nanoparticles were synthesized as the active targeting nanoparticle for LFA-1 expressing cells. The results showed a correlation between the level of LFA-1 and the degree of cellular uptake in the four different types of leukemic cell lines. Therefore, the cIBR peptide selectivity to different leukemic cell types was demonstrated in this study [10].

LFA-1 is the integrin adhesion molecule with 2 membrane-spanning subunits: alpha and beta chains [11], [12]. LFA-1 interacts with the Ig-like super family of proteins but its major ligand is intracellular adhesion molecule-1 (ICAM-1). LFA-1 mediated adhesion to cells, and to the extracellular matrix (ECM), is important in regulating leukocyte adhesion and T cell activation. LFA-1 is exclusively expressed on leukocyte cells, which is found on lymphoid cells of both T and B lineages and on a large proportion of bone marrow cells (~50%) [13], but not on exudated macrophages or non-lymphoid tissues [14]. It is absent, or presenting low levels on myeloid, erythroid precursor, and nonhematopoietic cells [15], [16]. In the physiological condition, there are 15,000 to 40,000 LFA-1 surface sites per peripheral lymphocyte, with more plentiful expression on T than B lymphocytes, and with increased expression on T blast cells [15]. Thus, it is beneficial for active targeting treatment in leukocyte-related diseases. On the other hand, the LFA-1 expression on cancer cells was reported in higher levels than on normal leukocyte. Chigaev *et al*. reported that the expression of LFA-1 on the human histiocytic lymphoma cell line (U937) was 90,000-130,000 sites per cell and the human lymphoblastoid cell line (JY) was 200,000-250,000 LFA-1 sites per cell [17].

cIBR peptide, a promising moiety for LFA-1 receptor, is the cyclo (1,12) PenPRGGSVLVTGC that is derived from residues of 1-21 in domain 1(N terminus) of ICAM-1. It was

World Academy of Science, Engineering and Technology
International Journal of Pharmacological and Pharmaceutical Sciences
Vol:6, No:6, 2012

proven to have the closest affinity with and specificity properties of LFA-1 when compared to the other synthesized peptides in the studies [18], [19]. Recently, cIBR has been coupled with PLGA nanoparticles (cIBR-NPs) for targeting lymphoblastic leukemic T cells [12] resulting in the rapid internalization of cIBR-NPs *via* receptor-mediated endocytosis by the LFA-1 expressing cell line. In addition, cIBR-NPs blocked the adhesion of T cells to lung epithelial cells generating a high level of ICAM-1 [12] and blocked T cell conjugation to dendritic cells more efficiently than untargeted nanoparticles (NPs), free peptides, and antibodies [20]. Due to the delivery of cIBR-NPs to LFA-1 on the targeted cell takes place the receptor-ligand recognition between the cIBR peptide and LFA-1. Thus the level of LFA-1 on targeted cell is the main factor to be considered to be an appropriate treatment of cIBR-conjugated PLGA nanoparticles. However, our previous study reported different levels of LFA-1 in four types of leukemic cell lines and a correlation between the level of expression and the degree of uptake but no studies have reported a correlation between the level of expression and the selectivity of active targeting carrier between cancer cells versus normal leukocyte cells. Therefore, it is important to prove the level of expression of LFA-1 and the selectivity of the cIBR-NPs of the LFA-1 high expressing leukemic cells and normal leukocytic cells. This can lead to a safety profile of the developed drug delivery system through avoiding the unnecessary effect on LFA-1 normal expressing cells.

In this study, LFA-1 was chosen to be used as the target receptor on the leukemic cells for active targeting nanoparticles, on which the cIBR peptide was conjugated to the surface of the PLGA nanoparticles. This was to study the selectivity of cIBR-conjugated PLGA nanoparticles, in the terms of binding and internalization, by PBMCs (normal cell), Mixed PBMC-Molt-3 cells (model of cell combination), and human lymphoblastic leukemia cell line (Molt-3 cells). The level of LFA-1 expression was determined in the PBMCs from ten healthy subjects, Mixed PBMC-Molt-3 cells (the combination of PBMCs and Molt-3 cells with ratio of 1:1), and Molt-3 cells. Comparison of selectivity in cIBR-NPs was evaluated by the degree of binding and internalization by these cell types. Herein, we have reported the ability of fabricated cIBR-PLGA nanoparticles to target leukemic cells rather than normal cells. The binding of cIBR-NPs by PMA activated and non-activated cells were examined. The related information such as levels of LFA-1 expression, nanoparticle characteristics, binding, and internalization of delivery devices were also discussed. Results from this study may be used to improve the efficacy of drug carrier for selective delivery to targeting cell.

## II. MATERIALS AND METHODS

### A. Materials

cIBR peptide (cyclo(1,12)-Pen-PRGGSVLVTGC-OH) (Mw 1,174.5) was synthesized on a Pioneer peptide synthesizer (PerSeptive Biosystems, CA). Poly (DL-lactic-coglycolic acid) (50:50) with terminal carboxylate group (PLGA, inherent viscosity 0.67 dL/g, Mw ~90 kDa) was purchased from LACTEL Absorbable Polymers International (Pelham, AL, USA). Pluronic F-127 was purchased from O-BASF The chemical company (St. Louis, MO, USA). 1-Ethyl-3-[3-dimethylaminopropyl] carbodiimide hydrochloride (EDC), N-hydroxysuccinimide (NHS), and Phorbol 12-myristate 13-acetate (PMA) were purchased from Sigma-Aldrich. (St. Louis, MO, USA). Coumarin-6 was obtained from Polysciences, Inc. (Warrington, PA, USA). RPMI 1640 medium was purchased from Invitrogen Cooperation (Grand Island, NY, USA). Bovine serum albumin (BSA) was purchased from Fluka Biochemika (St. Louis, MO, USA). Monoclonal anti-human CD11 (anti LFA-1) was purchased from Ancell (Bayport, MN, USA). Tris base was purchased from Fisher ChemAlert (Fair Lawn, NJ, USA). Mannitol was obtained from May and Beaker LTD. (Dagenham, Essex RM10 7XS, UK). Dialysis membrane (MWCO 12,000-14,000) was purchased from Membrane Filtration Products Inc. (Seguin, Texas, USA). Molt-3 cells were obtained from American Type Culture Collection (Manassas, VA, USA). Rabbit polyclonal anti CD11a was purchased from Abcam (Cambridge, UK). Horseradish peroxidase (HRP)-conjugated sheep anti-rabbit IgG antibody was obtained from Promega (Madison, WI, USA). SuperSignal® West Pico Chemiluminescent was purchased from Pierce (Rockford, IL, USA). Polyvinylidine fluoride transfer membrane was purchased from Pall Corporation (Pensacola, FL, USA). Prestained protein ladder was purchased from Fermentas (Hanover, MD, USA).

### B. Methods

#### 1. Cell Line

Molt-3 cells were cultured in suspension in RPMI 1640 medium supplemented with 10% (v/v) fetal bovine serum, 100 units/ml of penicillin, and 100 µg/ml of streptomycin in a humidified 37°C incubator with 5% $CO_2$ atmosphere.

#### 2. *Isolation* of Peripheral Blood Mononuclear Cells (*PBMCs*)

In this study, peripheral blood mononuclear cells represent normal cells for studying the LFA-1 expression, cIBR-NPs binding and uptake by the PBMCs as compared to those of the leukemic cell line (Molt-3 cells). PBMCs were taken as normal cells instead of the lymphocytes, which have been reported to express LFA-1. Peripheral blood samples were taken from healthy volunteers (8 female and 2 male) into sterile, pyrogen-free disposable syringes with endotoxin-free heparin (200 i.u./u.i./40 µl). Isolation of PBMCs from the subjects was performed using standard density gradient centrifugation (Lymphoprep™) (Axis-Shield PoC AS, Rodeløkka, Oslo, Norway). In brief, PBMCs were washed, resuspended and cultured in serum-free RPMI 1640 medium containing 0.5% L-glutamine and 1% penicillin-streptomycin. After 24 h incubation at 37°C, cells were washed and adjusted with the serum-free medium, at $2 \times 10^7$ cells/ml.

World Academy of Science, Engineering and Technology
International Journal of Pharmacological and Pharmaceutical Sciences
Vol:6, No:6, 2012

### 3. Mixed PBMC-Molt-3 Cells

In this work, PBMCs and Molt-3 cells, with a ratio of 1:1 were generated to imitate the condition that composed of normal cells and tumor cells (Mixed PBMC-Molt-3 cells). After 24 h of incubation, PBMCs and Molt-3 cells were seeded into 96-well tissue culture plate. The cell density of each cell type, in each well, was $2.5 \times 10^5$ cells per well in 5.0 ml serum free medium.

### 4. LFA-1 Expression

Two methods; flow cytometry and Western blotting, were included in the determination of LFA-1 expression for each cell sample. Different principles and techniques of these two methods were employed to confirm each other. For flow cytometry, the signal specificity depends on the antibody whereas the Western blotting assay depends on the antibody and molecular weight. A critical issue for using antibodies to measure a protein with flow cytometry is the reliability of quantitative measurements. To evaluate the quantitative reliability, the LFA-1 expressions on these cells were analyzed using Western blotting, and compared the results of parallel samples analyzed using flow cytometry.

#### i. Flow Cytometry

In order to verify the relationship between the degree of LFA-1 expression and nanoparticles uptake, the relative expression of LFA-1 on PBMCs, Mixed PBMC-Molt-3 cells, and Molt-3 cells were quantified in this study. Cells were washed three times with phosphate buffer saline (PBS; pH 7.4) and resuspended in serum free RPMI 1640. Cells ($5 \times 10^6$ cells/ml) were then added with normal AB serum (25 µl) and incubated, at 4°C, for 10 min to block non–specific binding. After that, cells were reacted with anti LFA-1-FITC (0.1 mg/ml) at 4°C for 45 min. Excess antibodies were removed by centrifugation at 3,000 rpm for 90 sec, and washed three times with cold 0.1% BSA in PBS. Finally, cells were fixed with 4% paraformaldehyde. The fluorescent intensity was determined using a FACscan flow cytometer. Data analysis was performed using Cell Quest software (BD Bioscience, San Jose, CA, *USA).*

#### ii. Immunoblotting for LFA-1 Receptor Expression

To confirm the results from the flow cytometry, the immunoblotting assay was used to determine the level of LFA-1 on each cell type. Cells were activated with 0.4 µM of PMA, in serum free media, for 24 h. After 24 h, cells ($1 \times 10^7$ cells) were lysed in RIPA buffer (25 mM Tris•HCl, pH 7.6, 150 mM NaCl, 1% NP-40, 1% sodium deoxycholate, 0.1% SDS) containing protease inhibitors. Cell lysates of PBMCs from three volunteers (No.1, 2, and 3) and Molt-3 cells were collected by centrifugation at 10,000 rpm for 15 min, at room temperature. The protein concentrations were measured by the Bradford method and standardized with BSA. Fifty micrograms of crude proteins were separated by SDS-PAGE and transferred to a polyvinylidene fluoride (PVDF) membrane. The membrane was blocked by 5% non-fat dry milk in PBS containing 0.1% Tween 20 (Solon Ind. Pkwy,

Solon, OH, USA), for 2 h and probed by 1 µg/ml anti-LFA antibody, for 3 h. The secondary antibody was added with the dilution of 1:10,000 for 2 h. Peroxidase activity was detected using SuperSignal® West Pico Chemiluminescent (Pierce, Rockford, IL, USA).

### 5. Preparation of Coumarin 6–Loaded PLGA Nanoparticles

Nanoparticles (NPs) encapsulating coumarin-6 were prepared using the solvent displacement method [12]. Coumarin 6 (0.05% w/v) and 40 mg PLGA were dissolved in 3 ml of acetone and sonicated for 15 min. This mixture was slowly dropped (17.6 ml/h) into the stirred aqueous solution containing 0.1% Pluronic F127 COOH (25 ml), anionic surfactant. Carboxylated Pluronic F127 was synthesized from hydroxylated Pluronic F127 according to the reported procedure [21]. After spontaneous formation of the NPs, organic solvent was evaporated by stirring for 6 h, at room temperature. Free coumarin-6 and excess Pluronic-COOH were removed by dialysis against 0.2% manitol solution, for 24 h. The size, size distribution, and zeta potential of PLGA nanoparticles encapsulating coumarin-6 were evaluated using photon correlation spectroscopy (PCS; Zetasizer® version 5.00, Malvern Instruments, UK).

### 6. Conjugation of cIBR Peptide to PLGA-Nanoparticles

Covalent coupling of carboxyl terminuses of modified Pluronic F127 on to the surface of PLGA nanoparticles with free amino acid terminus of cIBR peptide used EDC and NHS as coupling agents. Coumarin-6 loaded PLGA nanoparticles coated with Pluronic F-127-COOH (2.2 mg/ml) were buffered using 2-(N-morpholino) ethanesulfonic acid (MES, pH 6.5). Nanoparticles were then incubated, for 15 min with 100 mM EDC and 50 mM NHS. The activated carboxyl terminuses of Pluronic F127-COOH on the surface of nanoparticles were coupled with the amino terminus of the cIBR peptide (170 µmole) for 12 h, at room temperature. Conjugated NPs were collected by centrifugation (12,000 rpm, 10 min) and washed three times with purified water. The size, size distribution, and Zeta potential of cIBR-NPs were characterized using PCS.

### 7. Comparison of Cell Binding and Internalization of cIBR-NP between PMA activated and non-activated PBMCs

Two conditions of cells, as described above, were incubated with 0.4 µM of PMA in serum free media to stimulate the up-regulation of LFA-1 on the cell membranes, or without PMA in serum free media, for 24 h. Cells were washed three times and resuspened in an optimal volume of serum free media. Cells were seeded in 96-well plate which containing $CaCl_2$ (1.5 mM) at the density of $5 \times 10^5$ cells/well in 100 µl and then incubated with cIBR-NPs suspended in serum free medium (2.2 mg/70 µl) at 37°C for different time intervals (5, 30, and 60 min) to observe the particle uptake kinetics. Cells were then repeatedly centrifuged (2,200 rpm, 4°C for 2 min) and washed three times with cold PBS and fixed with 4% paraformaldehyde. The fluorescent intensities of cells were measured using the FACscan flow cytometer. Data analysis was performed using Cell Quest software.

World Academy of Science, Engineering and Technology
International Journal of Pharmacological and Pharmaceutical Sciences
Vol:6, No:6, 2012

### 8. In vitro Cellular Binding and Internalization of Nanoparticles

Cells ($5 \times 10^5$ cells/well) were seeded into a 96-well plate containing $CaCl_2$ (1.5 mM) in serum free medium and incubated with coumarin-6 encapsulated cIBR-NPs, or NPs without peptide-conjugation at the concentration of 2.2 mg/ml at 37°C, for 5, 30, and 60 min. Cell pellets were collected by centrifugation (2,200 rpm, 4°C for 2 min) and washed three times with cold 0.1% BSA in PBS to eliminate excess particles, which were not entrapped by cells and fixed with 4% paraformaldehyde. The fluorescent intensity was measured using FACscan flow cytometer. Data analysis was performed using Cell Quest software.

### 9. Statistical Analysis

Statistical evaluation of data was performed using an Analysis of Variance (one-way ANOVA). Newman–Keuls post-hoc test was used to assess where the significance of differences occurred. To compare the significant the differences between the means of the two groups an independent t-test was performed; in all cases, a value of $p < 0.05$ was accepted as the level of significance.

## III. RESULTS AND DISCUSSION

### A Determination of LFA-1 Expression on PBMCs, Molt-3 cells, and Mixed PBMC-Molt-3 Cells

#### 1. Flow cytometry

Because active targeting takes advantage of the molecular recognition as described above, the appropriate target should be carefully selected. The target receptor on the cancer cells should be overexpressed while lowered on normal cells. In this study, the relative expression of LFA-1 on PBMCs, Molt-3 cells, and Mixed PBMC-Molt-3 cells were quantitatively assessed using flow cytometry. After incubating these cells with anti-LFA-1-FITC for 45 min, the LFA-1 levels on the three cell conditions were analyzed using flow cytometry. The results showed that Molt-3 cells expressed a prominent degree of LFA-1 on cell surfaces with the mean fluorescent intensity (MFI) value of 73.68, compared to the PBMCs and Mixed PBMC-Molt-3 cells (27.01 and 37.09, respectively) (Fig. 1). The fluorescent intensity of Molt-3 cells, after reacting with anti–LFA-1–FITC, was ~2.73 and ~ 1.85-fold greater than PBMCs and Mixed PBMC-Molt-3 cells, respectively. For PBMCs and Mixed PBMC-Molt-3 cells, expression of LFA-1 levels was not significantly different. The average LFA-1 level on PBMCs, from the ten healthy volunteers, was ~63% which was less than the LFA-1 level on Molt-3 cells. It is not clear of the optimal level of receptor that should be used as a targeted receptor when comparing them to normal cells, but the greater difference in the level of LFA-1 is very beneficial for distinguishing the target cell from normal cells. Nevertheless, the binding and internalization ability of the drug carrier should be considered with the level of LFA-1 for the appropriation of active targeting drug carrier.
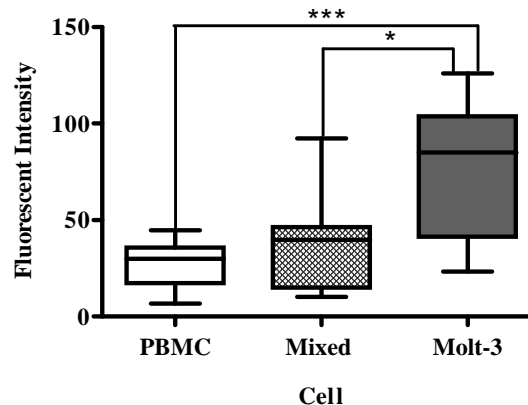


Fig. 1 Expression of LFA-1 on PBMCs, Molt-3 cells, and Mixed cells (Mixed PBMC-Molt-3 cells) after incubation with anti-LFA-1-FITC antibody. Data are given as median (n=10) and the error bars were calculated from stacked replicate. * indicates $p < 0.05$ and *** indicates $p < 0.001$

#### 2. Western Blotting for LFA-1 Receptor Expression

The presence of LFA-1 adhesion molecules on PBMCs and Molt-3 cells were investigated using Western blotting to support the results from the flow cytometry. Fig. 2 (a) showed that levels of LFA-1 protein were detected in activated and non-activated Molt-3 cells by PMA. The densitometric analysis revealed that the level of LFA-1 protein from activated and non- activated Molt-3 cells were not significantly different in the manner of $p < 0.05$. The LFA-1 protein level was detected in the low levels in activated and non-activated PBMCs comparing to Molt-3 cells (Fig. 2 (b)). The data also showed that there was more intensive LFA-1 protein level in Molt-3 cells when compared to PBMCs, supporting the results, from the flow cytometry, that PBMCs showed the low level of LFA-1 expression.

### B Preparation of Coumarin6–Loaded PLGA Nanoparticles

In the active targeting carrier, the targeting ligands were associated with functional group on surface of nanoparticles. The specific ligand of LFA-1, cIBR peptide, was reported to associate with the carboxylic group on surface of PLGA nanoparticles to improve the selectivity of the drug carrier to targeted cell [10]-[12]. The solvent displacement method was employed to prepare the carboxylated-PLGA nanoparticles. Coumarin-6, a fluorescent marker for the detection of the drug carrier when internalized to cells, was added into PLGA solution to form coumarin 6–loaded PLGA nanoparticles. The particle size, polydispersity index, and zeta potential of nanoparticles were characterized in Table I. The mean diameter of untargeted nanoparticles and cIBR conjugated nanoparticles were $196.8 \pm 5.8$ and $230.2 \pm 10.1$ nm, respectively.

World Academy of Science, Engineering and Technology
International Journal of Pharmacological and Pharmaceutical Sciences
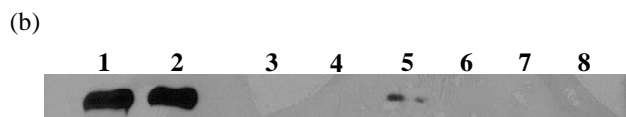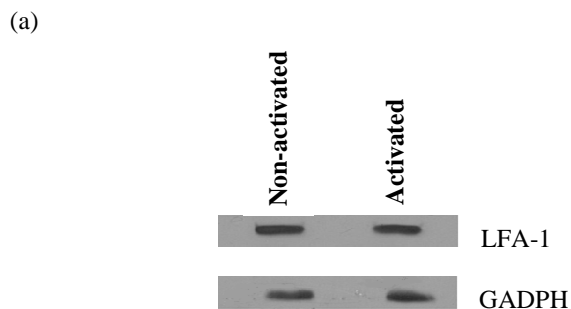Vol:6, No:6, 2012

(a)



(b)



Fig. 2 Whole cell lysates of PBMCs and Molt-3 expressing LFA-1 cells were resolved on 6.5% SDS-PAGE, transferred to a PVDF membrane and blotted with anti CD11a antibodies. (a) LFA-1 protein in activated and non-activated Molt-3 cells by 0.4 µM PMA for 24 h. (b) LFA-1 protein in activated Molt-3 cells (1), non-activated Molt-3 cells (2), activated PBMC; No.1 (3), non-activated PBMC; No.1 (4), activated PBMC; No.2 (5), non-activated PBMC; No.2 (6), activated PBMC; No.3 (7) and non-activated PBMC; No.3 (8) by 0.4 µM PMA. Each lane represents $1 \times 10^7$ cells and 50 µg of protein equivalents were loaded.

A low polydispersity index of 0.059 and 0.077 was obtained from both formulations indicating a narrow size distribution of the nanoparticles suspension, and consequently a homogenous distribution. Surface charge is an important element of stability of colloidal nanoparticles system in medium. The repulsion among the nanoparticles with same type of surface charge provides extra stability. The zeta potential of untargeted-NPs and cIBR-NPs were -29.5 and -39.4 mV, respectively. This may be due to the masking of anionic surface charges by Pluronic F-127 COOH coating. The physiochemical properties of drug carriers are the essential factors to predict the fate of system after administration. Particle size is an important parameter as it can directly affect the physical stability, cellular uptake, biodistribution, and drug release from the nanoparticles [22]

TABLE I
PROPERTIES OF NANOPARTICLES

| Nanoparticles | Mean size (nm) | Polydispersity index | Zeta potential value (mV) |
|---|---|---|---|
| untargeted NPs | 196.8 ±5.8 | 0.059 ± 0.09 | -29.5±3.23 |
| cIBR-NPs | 230.2 ± 10.1 | 0.077 ± 0.06 | -39.4±1.37 |

Values are given as mean ± S.D. (n=3)

### C. Conjugation of cIBR Peptide to PLGA Nanoparticles

The modifying surface characteristic can prevent particles uptake by the reticuloendothelial system (RES) but cannot assist nanoparticles to deliver exactly to the targeted site. Active targeting was employed to assist nanoparticles by attaching the targeting ligand to the nanopartice surface. In this study, the carbodiimide reaction was used in the covalent conjugation between the cIBR peptide and carboxylic group on the nanoparticles surface. The carboxyl group of Pluronic F-127 COOH was converted to an active carboxyl form by carbodiimide reagents (EDC and NHS). The active carboxyl groups on nanoparticles' surfaces were coupled with free amino groups in cIBR peptides to form amide bonds for this conjugation. After the reaction, free cIBR peptides were collected and assayed using HPLC-UV to determine density of peptides on the surface of nanoparticles. It was calculated by assuming a normal Gussian particles size distribution. The density of cIBR value was $36.9 \pm 4.5$ pmol/cm$^2$, with the particle size, and total surface area were 230.2 nm and 0.0389 m$^2$/g of PLGA, respectively (Table II).

TABLE II
DENSITY OF PEPTIDES ON THE SURFACE OF NANOPARTICLES

| | Size (nm) | Total surface area (m$^2$/g of PLGA) | Density of cIBR (pmol/cm$^2$) |
|---|---|---|---|
| cIBR-NPs | 230.2 | 0.0389 | 36.9 ± 4.5 |

Values are representative of three experiments (mean ± S.D.)

### D. Comparison of Cell Binding and Uptake of cIBR-NP between PMA activated and non-activated cells

LFA-1 switches from the inactive to the active form to bind to ICAM-1 by either inside-out or outside-in activation [23], [24]. Inside-out activation of LFA-1 is induced by chemokine activation of G-protein coupled receptors [23] and can be mediated by the use of PMA. The outside-in activation of β2 and other integrins is a method for ligand-induced (leukocyte, LFA-1) to modulate signaling pathways within a cell [24]. PMA was previously reported to activate protein kinases C (PKC) via the phosphorylation of the β2-linked proteins Rack1 (receptor for activated PKC) and MacMARCKS (macrophage-enriched myristolated alanine-rich C kinase substrate), a member of the MARCKS family of PKC substrates, leading to the forming of high avidity clusters of LFA-1 [12]. Anderson et al. reported that the expression of LFA-1 was not enhanced by PMA exposure [25]. Thus, the effect of PMA on cellular uptake was investigated on the function of LFA-1 upon the cellular uptake of cIBR-NPs. For PBMCs, the result presented the significant difference in cellular uptake between PMA activated and non-activated cells, at 5 min. Beyond 30 min, the profile of uptake in both cells were similar (Fig. 3). On the other hand, the similar trend of uptake between activated and non-activated cells was found in Mixed PBMC-Molt-3 cells at all time points (Fig. 4). An incubation time of 60 min, the cellular uptake of cIBR-NPs by activated Molt-3 cells was significantly different from the non-activated Molt-3 cells but the cellular uptake profiles within 60 min were similar ($p<0.05$) (Fig. 5). Since, the PMA activation of the cIBR binding is time-dependent [25], it may help to explain the difference in the percent uptake of cIBR-NPs between activated and non-activated Molt-3 cells, at 60 min. The effect of PMA on the cellular uptake of cIBR-NPs by LFA-1 expressing cells may not be clear but the ability of cIBR-NPs binding to the non-activated cells may be due to the appearance of Ca$^{2+}$ in the medium that binds to the metal ion-dependent binding site (MIDAS) of LFA-1 to keep LFA-1 in the closed conformation and cIBR peptide preferentially binding to the closed from of LFA-1 [25]. cIBR peptide

World Academy of Science, Engineering and Technology
International Journal of Pharmacological and Pharmaceutical Sciences
Vol:6, No:6, 2012

containing Pro-Arg-Gly (PRG) sequence [18], [26], [27] is recognized by LFA-1 and the ICAM-1 interaction with LFA-1 can be mimicked by strongly binding to LFA-1 cluster [28]. It may control the conformation change of I-domain of LFA-1 [25]. This information helps to support the uptake-ability of cIBR-NPs by LFA-1 expressing cells in the PMA-lacking condition.
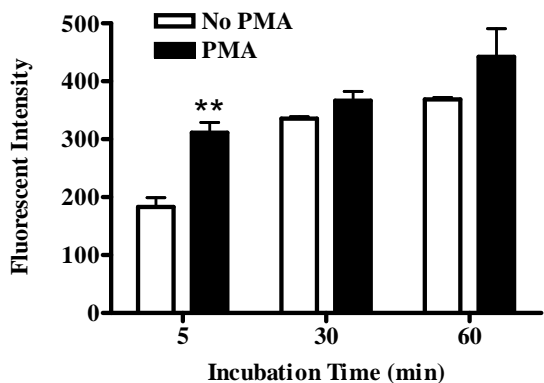


Fig. 3 The influence of the conformation of LFA-1 on the uptake of cIBR-NPs by activated PBMCs (black) and non-activated PBMCs (white) from three healthy subjects. Data are given as mean ± S.D. (n=3); ** indicates $p<0.01$
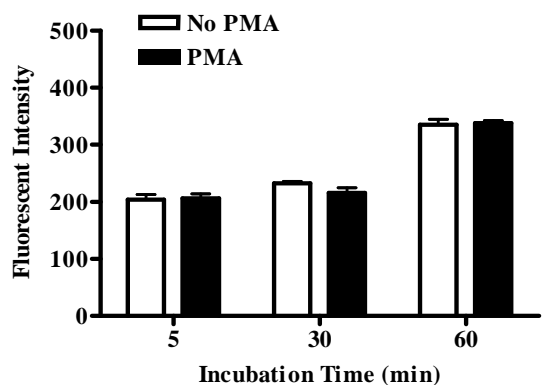


Fig. 4 The influence of the conformation of LFA-1 on the uptake of cIBR-NPs by activated Mixed PBMC-Molt-3 cells (black) and non-activated Mixed PBMC-Molt-3 cells (white). Data are given as mean ± S.D. (n=3)

*E. In vitro Cellular Binding and Internalization of Nanoparticles*

The aim of active targeting was to improve the cellular binding and internalization of nanocarrires. Thus, binding and internalization of the cIBR-NPs and untargeted NPs to each different cell type is our goal to prove the selectivity of cIBR-NPs.
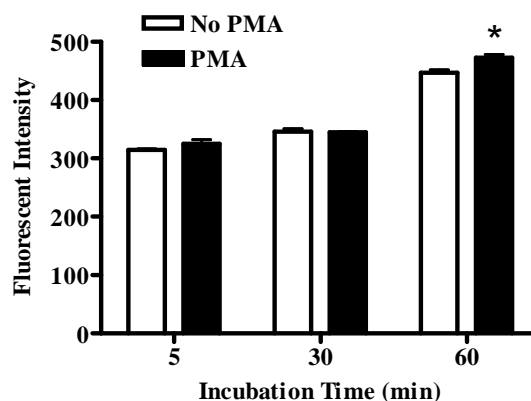


Fig. 5 The influence of the conformation of LFA-1 on the uptake of cIBR-NPs by activated Molt-3 cells (black) and non-activated Molt-3 cells (white). Data are given as mean ± S.D. (n=3); * indicates $p<0.05$

After incubation of the cIBR-NPs and untargeted NPs with three cell conditions, at 5, 30, and 60 min, cellular binding and internalization of both formulations were investigated using a flow cytometer. The increase of fluorescent intensities of NPs treated cells related to that of the untreated control cells was expressed as mean fluorescent intensities of NPs treated cells related to that of the untreated control cells was expressed as mean fluorescent intensity, relative to the control. The florescences from both cIBR-NPs and untargeted NPs internalized in cells were shown in Fig. 6, Fig.7, and Fig. 8. The significant fluorescent difference between cIBR-NPs and untargeted NPs can be clearly determined in all cell types. The fluorescent intensity of cIBR-NPs in cells was higher than untargeted NPs at all time points (5, 30, and 60 min) with the range of 1.60-2.73-fold in three cell conditions. The greater amount of cIBR-NPs in the cells indicated the enhanced internalization and retention effect of the targeted carrier *via* ligand-receptor endocytosis, indicating that cIBR-NPs were better target than nanoparticles without cIBR conjugation. Without targeting ligand, the untargeted NPs could enter the cells and diffuse away from the cells over time. The fluorescent intensities of Molt-3 cells after 5 min of incubation, with cIBR-NPs were higher than those of PBMCs and Mixed PBMC-Molt-3 cells by ~2.44 and ~1.5-fold, respectively, indicating that the uptake activity of Molt-3 cells occurred more rapidly than in PBMCs and Mixed PBMC-Molt-3 cells (Fig. 10). Moreover, the results also showed the prominent binding and internalization of cIBR-NPs in Molt-3 cells at all time points when compared to those of PBMCs. This suggests that the binding and internalization capacity of cIBR-NPs by Molt-3 cells was more specific and sufficient than PBMCs, due to the low LFA-1 level on the membrane of PBMCs (normal cells). The cIBR-NPs targeted to the PBMCs had a low capacity for binding and internalization, suggesting that the targeting and safety profile of cIBR-NPs is in the high and low level of LFA-1 on their cell membranes. In comparison to the binding and internalization between Mixed PBMC-Molt-3 cells and Molt-3 cells, except 30 min, the profile of uptake of cIBR-NPs showed no significant difference when compared to the fluorescent intensity of

World Academy of Science, Engineering and Technology
International Journal of Pharmacological and Pharmaceutical Sciences
Vol:6, No:6, 2012

Mixed PBMC-Molt-3 cells to Molt-3 cells. Additionally, the results were parallel, in the same direction, with LFA-1 level, which Molt-3 cells showed to have the highest LFA-1 levels on the cell surface membrane, and the highest cellular binding and internalization. Similarly, PBMCs showed the low levels of LFA-1 expression, cellular binding and internalization of cIBR-NPs were also presented in the lowest degree. It was suggested that the degree of expression of LFA-1 involved in the level of binding and internalization of cIBR-NPs, in LFA-1 expressing cell. Taking the linear regression line, the rate of cellular binding and internalization was presented in the terms of a slope. Interestingly, the slope of Molt-3 cells showed the highest values for both the untargeted NPs and cIBR-NPs, indicating the highest rate of binding and internalization of with the values of 4.67 and 11.69 FI/min, respectively, when compare to other cells (Fig. 9 and Fig. 11). In comparison to the slope between untargeted NPs and cIBR-NPs, the results demonstrated that the slope of cIBR-NPs were ~ 2.33, 4.43, and 1.93-fold greater than those of untargeted NPs in Molt-3 cells, Mixed PBMC-Molt-3 cells, and PBMCs, respectively. It was suggested that the binding and internalization of cIBR-NPs were more rapid than untargeted NPs. The result confirmed that targeting of cIBR peptide conjugation nanoparticles is significant and effective for LFA-1 overexpressing cells.
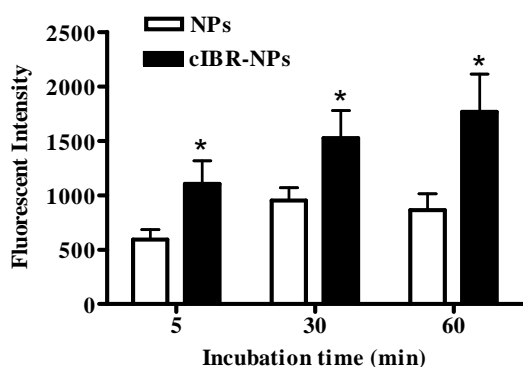


Fig. 6 The comparison between the binding and internalization of cIBR-NPs and NPs after incubation with Molt-3 cells. Results are given as mean ± S.D. (n=10); * indicates $p<0.05$
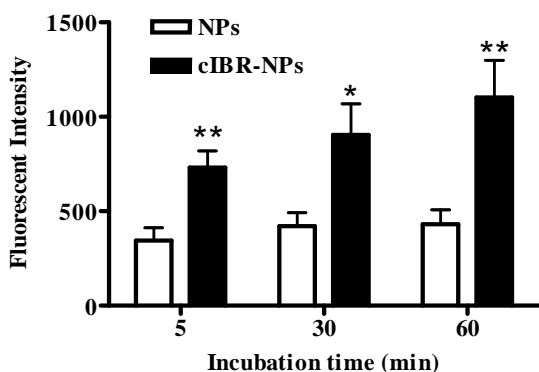


Fig. 7 The comparison between the binding and internalization of cIBR-NPs and NPs after incubation with Mixed PBMC-Molt-3 cells.Results are given as mean ± S.D. (n=10); * indicates $p<0.05$ and ** indicates $p<0.01$
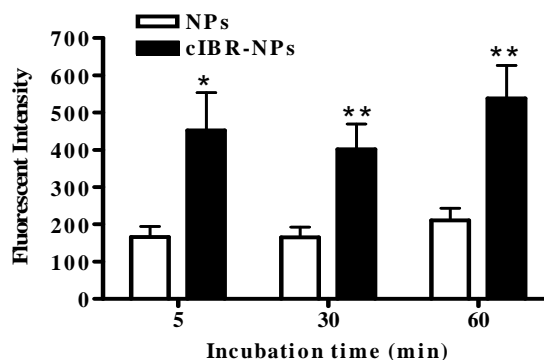


Fig. 8 The comparison between the binding and internalization of cIBR-NPs and NPs after incubation with PBMCs. Results are given as mean ± S.D. (n=10); * indicates $p<0.05$ and ** indicates $p<0.01$
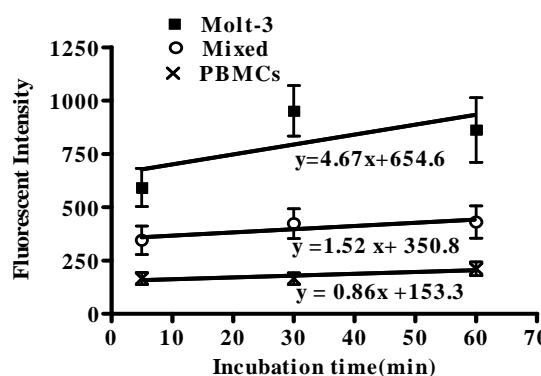


Fig. 9 Linear regression line of untargeted NPs binding profiles by PBMCs, Molt-3 cells, and Mixed PBMC-Molt-3 cells
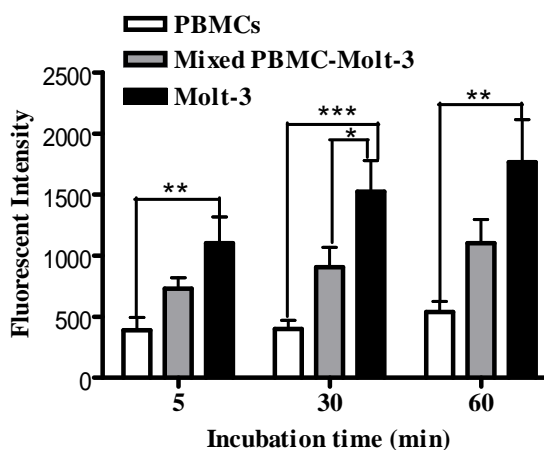


Fig. 10 Kinetic binding profiles of cIBR-NPs by PBMCs, Molt-3 cells, and Mixed PBMC-Molt-3 cells after incubation for 5, 30, and 60 min. Data represents mean ± S.D.(n=10); * indicates $p<0.05$, ** indicates $p<0.01$ and *** indicates $p<0.001$.

World Academy of Science, Engineering and Technology
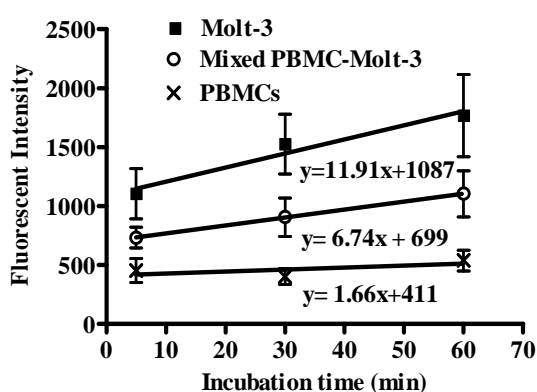International Journal of Pharmacological and Pharmaceutical Sciences
Vol:6, No:6, 2012

Fig. 11 Linear regression lines of cIBR-NPs binding profiles by PBMCs, Molt-3 cells, and Mixed PBMC-Molt-3 cells

## IV. CONCLUSIONS

PLGA nanoparticles and cIBR coupled PLGA nanoparticles have been formulated *via* solvent displacement method. The results of cellular uptake of cIBR-NPs showed an increase in nanoparticle uptake in LFA-1 expressing cells as compared to untargeted nanoparticles using flow cytometry. Moreover, the results demonstrated the correspondence of LFA-1 expression level and the cellular uptake of cIBR-NPs. Molt-3 cells presented the highest degree of LFA-1 expression, and exhibited the highest degree of cIBR-NPs binding. PBMC was represented as the normal cell model in this study, for comparing the selectivity of cIBR-NPs versus leukemic cell line (Molt-3 cells). PBMCs showed the lowest degree of LFA-1 expression, and the lowest cellular uptake of the targeted carrier when compare to the other cells, indicating the selectivity and safety profile of cIBR-NPs when exposed to the different LFA-1 levels on various cell types. These studies suggest that cIBR peptides assist in improving the specificity of nanocarriers as the targeting moiety. The cIBR conjugated PLGA nanoparticles system was proven to be an attractive candidate of nanocarriers for detecting and targeting LFA-1 on leukemic cells, minimizing effect on healthy cells. The obtained information may be useful for systemic delivery of target NPs to patients with other kinds of cancer, with possible disseminated tumors, in the future.

## REFERENCES

[1] Hino M, *et al.* Leptin Receptor and Leukemia. *Leukemia Lymphoma* 2000; 36(5-6):457-461.
[2] Stirewalt DL & Radich JP The role of FLT3 in haematopoietic malignancies. *Nat Rev Cancer* 2003; 3(9):650-665.
[3] DiJoseph J, Dougher M, Armellino D, Evans D, & Damle N Therapeutic potential of CD22-specific antibody-targeted chemotherapy using inotuzumab ozogamicin (CMC-544) for the treatment of acute lymphoblastic leukemia. *Leukemia* 2007; 21(11):2240-2245

[4] Bächli EB, Schaer DJ, Walter RB, Fehr J, and Schoedon G. Functional expression of the CD163 scavenger receptor on acute myeloid leukemia cells of monocytic lineage. *J Leukocyte Bio* 2006; 79(2):312-318.
[5] Rock KL, Benacerraf B, and Abbas AK. Antigen presentation by hapten-specific B lymphocytes. I. Role of surface immunoglobulin receptors. *J Exp Med* 1984; 160(4):1102.
[6] Horst E, *et al.* Expression of the leucocyte integrin LFA-1 (CD11a/CD18) and its ligand ICAM-1 (CD54) in lymphoid malignancies is related to lineage derivation and stage of differentiation but not to tumor grade. *Leukemia: official journal of the Leukemia Society of America, Leukemia Research Fund, UK* 1991; 5(10):848.
[7] Medeiros LJ, *et al.* Expression of LFA-1 in non-hodgkin's lymphoma. *Cancer* 1989; 63(2):255-259
[8] Phongpradist R, *et al.* LFA-1 on Leukemic Cells as a Target for Therapy or Drug Delivery. *Curr Pharm Design* 2010; 16(21):2321-2330
[9] Woessner S, *et al.* Expression of lymphocyte function-associated antigen (LFA)-1 in B-cell chronic lymphocytic leukemia. *Leukemia Lymphoma* 1994; 13(5):457-461
[10] Chittasupho C, Manikwar P, Krise J, Siahaan T, and Berkland C. cIBR Effectively Targets Nanoparticles to LFA-1 on Acute Lymphoblastic T Cells. *Mol Pharm* 2009; 7(1):146-55
[11] Wacholtz MC, Patel S, and Lipsky P. Leukocyte function-associated antigen 1 is an activation molecule for human T cells. *J Exp Med* 1989; 170(2):431.
[12] T. Hilden, *Affinity and Avidity of the LFA-1 Integrin is Regulated by Phosphorylation*, Faculty of Bioscience, University of Helsinki, 2005, pp. 9-24
[13] Springer TA, Dustin ML, Kishimoto TK, and Marlin SD. The lymphocyte function associated LFA-1, CD2, and LFA-3 molecules: cell adhesion receptors of the immune system. *Annu Rev Immunol* 1987; 5(1):223-252.
[14] Miller BA, Antognetti G, and Springer T. Identification of cell surface antigens present on murine hematopoietic stem cells. *J Immunol* 1985; 134(5):3286.
[15] Chigaev A, *et al.* Real-time Analysis of the Inside-out Regulation of Lymphocyte Function-associated Antigen-1 Revealed Similarities to and Differences from Very Late Antigen-4. *J Biol Chem* 2011; 286(23):20375
[16] Anderson M, Yakovleva T, Hu Y, and Siahaan TJ. Inhibition of ICAM-1/LFA-1-mediated heterotypic T-cell adhesion to epithelial cells: design of ICAM-1 cyclic peptides. *Bioorg Med Chem Lett* 2004; 14(6):1399-1402
[17] Zimmerman T, *et al.* ICAM-1 Peptide Inhibitors of T-cell Adhesion bind to the allosteric site of LFA-1. An NMR Characterization. *Chem Biol Drug Des* 2007;70(4):347
[18] Chittasupho C, Shannon L, Siahaan TJ, Vines CM, & Berkland C. Nanoparticles Targeting Dendritic Cell Surface Molecules Effectively Block T Cell Conjugation and Shift Response. *ACS Nano* 2011; 5(3):1693-1702
[19] Chittasupho C, *et al.* ICAM-1 targeting of doxorubicin-loaded PLGA nanoparticles to lung epithelial cells. *Eur J Pharm Sci* 2009; 37(2):141-150
[20] Mukerjee A and Viswanatha J. Formulation, Characterization and Evaluation of Curcumin-loaded PLGA Nanospheres for Cancer Therapy. *Anticancer res* 2009; 29(10):3867
[21] Carre o R, *et al.* A Mechanism for Antibody-mediated Outside-in Activation of LFA-1. *J Biol Chem* 2008; 283(16):10642
[22] Lub M, van Kooyk Y, & Figdor C. Ins and outs of LFA-1. *Immunol today* 1 1995; 6(10):479-483
[23] Anderson M, Tejo B, Yakovleva T, and Siahaan TJ. Characterization of binding properties of ICAM-1 peptides to LFA-1: inhibitors of T-cell adhesion. *Chem Biol Drug Des* 2006; 68(1):20
[24] Gürsoy R, Jois D, and Siahaan TJ. Structural recognition of an ICAM-1 peptide by its receptor on the surface of T cells: conformational studies of cyclo (1, 12)-Pen-Pro-Arg-Gly-Gly-Ser-Val-Leu-Val-Thr-Gly-Cys-OH. *J Pept Res* 1999; 53(4):422-431
[25] Anderson ME, Yakovleva T, Hu Y, and Siahaan TJ. Inhibition of ICAM-1/LFA-1-mediated heterotypic T-cell adhesion to epithelial cells: design of ICAM-1 cyclic peptides. *Bioorg Med Chem Lett* 2004; 14(6):1399-1402.
[26] Kim M, Carman CV, Yang W, Salas A, and Springer TA. The primacy of affinity over clustering in regulation of adhesiveness of the integrin αLβ2. *J Cell Biol* 2004;167(6):1241-1253

Open Science Index, Pharmacological and Pharmaceutical Sciences Vol:6, No:6, 2012 publications.waset.org/6057.pdf

[27] Anderson ME, Yakovleva T, Hu Y, Siahaan TJ. Inhibition of ICAM-1/LFA-1-mediated heterotypic T-cell adhesion to epithelial cells: design of ICAM-1 cyclic peptides. *Bioorg Med Chem Lett* 2004;14(6):1399-402

[28] Kim M, Carman CV, Yang W, Salas A, Springer TA. The primacy of affinity over clustering in regulation of adhesiveness of the integrin αLβ2. *J Cell Biol* 2004; 167(6):1241-53.